Design of Microstereolithography System Based on Dynamic Image Projection for Fabrication of Three-Dimensional Microstructures

Jae Won Choi, Young Myoung Ha
Department of Mechanical and Intelligent Systems Engineering, Pusan National University, San 30 Jangjeon-dong, Geumjeong-gu, Busan 609-735, Korea
Seok Hee Lee*
School of Mechanical Engineering, Pusan National University, San 30 Jangjeon-dong, Geumjeong-gu, Busan 609-735, Korea
Kyung Hyun Choi
Department of Mechatronics Engineering, Cheju National University, Jejudaehakno, Jeju-si, Jeju-do 690-756, Korea

As demands for complex microstructures with high aspect ratios have increased, the existing methods, MEMS and LIGA, have had difficulties coping with the number of masks and fabricable heights. A microstereolithography technology can meet these demands because it has no need of masks and is capable of fabricating high aspect ratio microstructures. In this technology, 3D part is fabricated by stacking layers, 2D sections, which are sliced from STL file, and the Dynamic Image Projection process enables the resin surface to be cured by a dynamic image generated with DMD™ (Digital Micromirror Device) and one irradiation. In this paper, we address optical design process for implementing this microstereolithography system that takes the light path based on DMD operation and image-formation on the resin surface using an optical design program into consideration. To verify the performance of this implemented microstereolithography system, complex 3D microstructures with high aspect ratios were fabricated.

Key Words : Microstereolithography, Microstructures, Digital Micromirror Device (DMD), Curing

1. Introduction

Nowadays demands for ultra-precise parts such as micro-mechanical parts, information and communication devices, and medical devices are increasing. MEMS and LIGA technology have met these demands for a long time, but they have technical limitations when fabricating complex 3D parts or devices with high aspect ratios. Microstereolithography technology has been studied and developed to overcome these limitations, although it has weakness about fabricable material in comparison with MEMS and LIGA. The microstereolithography process is most similar to the conventional stereolithography process and uses the same input format, STL. A final part is fabricated by slicing a modeling part, generating a machining path, and stacking each fabricated layer sequentially. There are two types of microstereolithography system, scanning and projection, that can be used in curing method (Varadan et al., 2001).

In scanning method as shown in Fig. 1, the part

* Corresponding Author,
E-mail : sehlee@pusan.ac.kr
TEL : +82-51-510-2327; **FAX** : +82-51-514-0685
School of Mechanical Engineering, Pusan National University, San 30 Jangjeon-dong, Geumjeong-gu, Busan 609-735, Korea. (Manuscript **Received** March 31, 2006; **Revised** August 30, 2006)

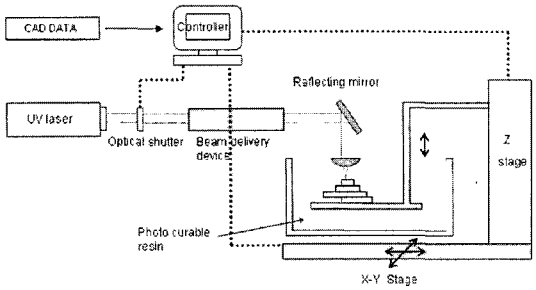

Fig. 1 Schematic of scanning microstereolithography

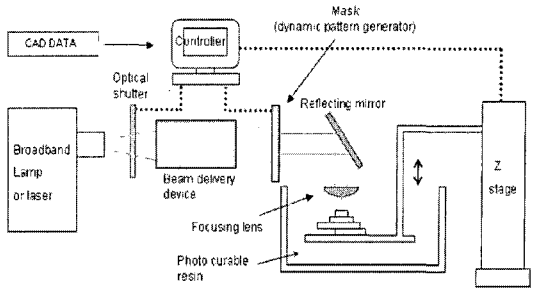

Fig. 2 Schematic of projection microstereolithography

is produced by stacking each fabricated layer using focused beam spot control on the resin surface according to the sliced section shape. The X-Y stage is usually used for scanning the focused beam spot, and the Z stage is used for stacking the fabricated layers. In 1993, Ikuta and Hirowatari (1993) reported the development of the first type of microstereolithography called Integrated Harden polymer process (IH process) and this system have been continuously upgraded (Ikuta et al., 1996; 1998; 1999). The fabrication resolution is almost several μm wide and deep. The latest system that was developed is called a two-photon IH process that uses two-photon absorption and can usually fabricate microstructures with resolution of hundreds nm in the μm range (Maruo et al., 2003; Park et al., 2005; 2006). Using similar scanning microstereolithography systems, unique microstructures have been fabricated and a variety of investigations have been conducted by several researchers around the world (Zhang et al., 1999, Sun and Zhang, 2002; Lee at al., 2004; Kim et al., 2005).

In projection method shown in Fig. 2, the part is produced by stacking fabricated layers using a technique similar to the scanning type. However, each layer is cured by dynamic mask and one irradiation from light source at a time. The Z stage is only used for stacking the fabricated layers. Projection microstereolithography can produce microstructures faster than the scanning type because it requires little time to scan with its focused beam spot. To make a dynamic pattern, LCD (Liquid Crystal Display) and DMD (Digital Micromirror Device) are used. In the mid 1990's, a projection microstereolithography system using LCD was first developed (Bertsch et al., 1997). An electric signal enables each pixel to be opened and closed on the LCD according to the desired pattern. This LCD projection microstereolithography system has been improved and is capable of producing a variety of microstructures with resolutions of several μm wide and deep (Farsari et al., 2000; Provin and Monneret, 2002; Oda et al., 2004). In the beginning the system's resolution was low because of the contrast produced by the LCD, but current systems have higher resolution due to improvements to LCD. DMD has been used in place of LCD as dynamic pattern generator due to its high contrast and resolution (Bertsch et al., 2000; Smith, 2004; Bertsch et al., 2004; Limaye, 2004; Sun et al., 2005; Choi et al., 2005). Each pixel on the DMD reflects incident light according to desired bitmap image. The resolution of the DMD microstereolithography system is a few μm and better than that of the LCD microtereolithography system. Especially, Sun et al. (2005) have been produced suspended beam with 600 nm diameter, which is the smallest feature among the reported projection based microstereolithography processes.

Above reported papers pass over optically designing and verifying the system for the reliability, though they employ a few resolutions and can fabricate microstructures. In this paper, we address the optical design process for implementing microstereolithography system by taking the light path based on the DMD operation and the focused image on the resin surface using an optical design program into consideration. The optical

design process consists of two parts ; illumination to produce a uniform light intensity on DMD surface and image-formation to produce a focused image on the resin surface. To verify the optical design, the light intensity is measured and the 2D patterns are fabricated. The fabricated 2D patterns are observed using a microscope. Finally, a few complex 3D microstructures with high aspect ratios are fabricated to verify the performance of the implemented microstereolithography system.

2. Microstereolithography System Based on Dynamic Image Projection

2.1 Components

The microstereolithography apparatus suggested in this paper as shown in Fig. 3 consists of illumination part, a dynamic pattern generator, image-formation parts, and a Z stage. The illumination part that consists of light source, filter, an electric shutter, a collimating lens, and a reflecting mirror plays a role in producing a uniformly intense light on DMD. The light source is a mercury lamp and with 200 W of output power. The light is filtered at 365 nm with ± 10 nm bandwidth using a metallic UV filter. The electric shutter switches the light on and off to transfer the desired energy. The collimating lens that is usually convex lens is used because the light emitted from the lamp diverges along the optical axis. Finally, the light has to be directed at the DMD surface according to reflecting angle.

The dynamic pattern generator plays an important role in the projection microstereolithography process. The fabrication time is shortened because each layer is cured by one irradiation using a dynamic pattern generator, which generates an image of the sliced section of the fabrication model by producing a black and white region similar to mask.

In this paper, DMD, which is made by Texas Instrument, Inc., is used to generate dynamic mask. It is shown in Fig. 4(a) and consists of 1024×768 micromirrors, which have sides of 13.68 μm. It only reflects the part to be cured by independently tilting each micromirror at $\pm 12°$. If a micromirror is tilted at $+12°$, the incident light is reflected to the tube and objective lens, but and if it is tilted at $-12°$, the incident light is reflected to the other position. Fig. 4(b) represents the reflected light direction by the tilt angle of one micromirror. The input signal is the bitmap to be cured and transferred to the DMD in sequence.

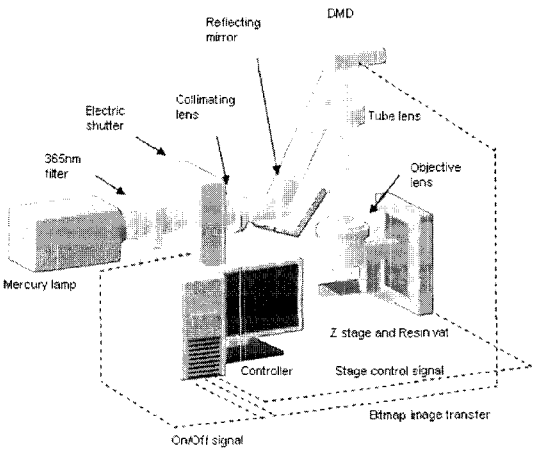

Fig. 3 Schematic of suggested microstereolithography system

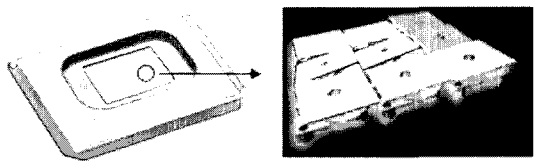

(a) Magnified micromirror

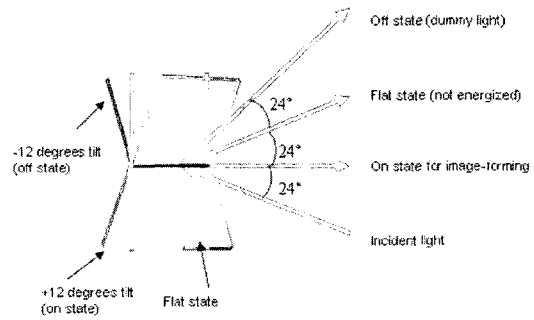

(b) Reflected light path according to mirror tilt

Fig. 4 Digital Micromirror Device

The light from DMD is reflected toward tube lens which is a UV achromat doublet lens with 120 mm focal length and delivers the beam to the objective lens. The objective lens is used to focus the patterned image on the resin surface. The Nu-

Table 1 Specifications of Z stage

Travel Range	50 mm
Resolution	0.1 μm
Repeatability	$\pm$0.1 μm
Position Accuracy	$\pm$0.3 μm
Maximum Speed	300 mm/s

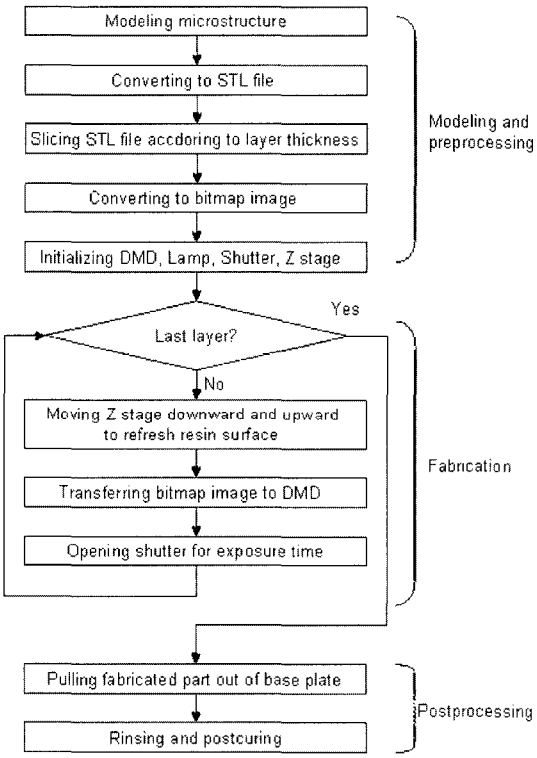

Fig. 5 Overall process in microstereolithography

merical Aperture (N.A.) and focal length of this lens are 0.45 and 10 mm, respectively.

Finally, to stack the fabricated layers, a high resolution Z stage is needed. One layer is fabricated by one irradiation, and then the Z stage moves down and up again to refresh the resin surface for the next curing. The specifications for the Z stage (ALS130-050, Aerotech) are shown in Table 1.

2.2 Overall process for fabrication of microstructures

The fabrication process in the microstereolithography apparatus is similar to that of the conventional SLA system. First of all, the part to be fabricated is modeled using CAD software, and it is converted to an STL file which consists of triangle facets. Section data, which are a closed loop, is generated by slicing the STL file into layer thickness, and the bitmap is generated for input to DMD. At this time, the bitmap image has to be bilateral symmetry about formed image because bilateral symmetry of the image on DMD is formed on resin surface. After generating the bitmap images for every layer, fabrication starts by initializing DMD, the lamp, the electronic shutter, and the Z stage. The Z stage stacks the layers that have already been fabricated, and the resin surface is refreshed by moving down and up according to the thickness of the layer. After refreshing the resin surface, the bitmap image is transferred to DMD, and the resin surface is cured by opening the shutter for the exposure time. After the process has been completed for every layer, the final fabricated part is produced. Fig. 5 shows the microstereolithography fabrication process.

3. Optical Design of Microstereolithography System

All of the components have to be installed at specified positions by taking the light path and image-formation into consideration. The process is divided into two parts: illumination and image-formation. For the illumination part, the incident light on the DMD surface has to have uniform intensity. For image-formation part, the patterned image on the DMD has to be delivered and focused on the resin surface with minimum distortion using tube and objective lens.

3.1 Illumination part

The illumination part is composed of a light source, an electronic shutter, a convex lens, a reflecting mirror, and DMD. The first goal is to produce incident light to be collimated before incidence on DMD. The second goal is to produce a principle ray of incident light on the optical axis of tube and objective lens so that the light is delivered perpendicularly on the resin surface. To achieve this purpose, every component needs to

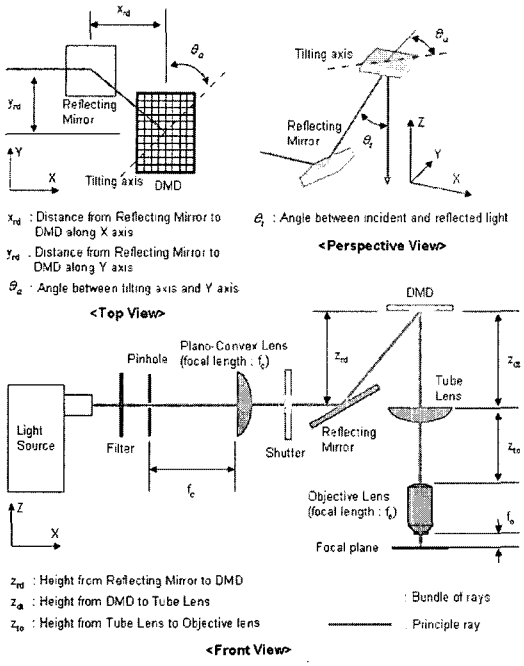

x_{rd} : Distance from Reflecting Mirror to DMD along X axis
y_{rd} : Distance from Reflecting Mirror to DMD along Y axis
θ_a : Angle between tilting axis and Y axis
θ_t : Angle between incident and reflected light
z_{rd} : Height from Reflecting Mirror to DMD
z_{dt} : Height from DMD to Tube Lens
z_{to} : Height from Tube Lens to Objective lens

Fig. 6 Component positions according to light path

be aligned along the principle ray of the light. To produce collimated light, the front focal point of convex lens (f_c=70 mm) is positioned at the first focal point from the light source as shown in Fig. 6. Also, the reflecting mirror has to be positioned after taking the height (z_{rd}) of DMD from the reflecting mirror, the tilt angle (θ_t) of the micromirror between incident and reflected light on DMD, and the tilt axis angle (θ_a) of the micromirror between the Y and tilt axis into consideration.

From Fig. 6, the position of the reflecting mirror can be derived using the values (z_{rd}, θ_t, θ_a) related to DMD. The positions of the tube (z_{dt}) and objective lens (z_{to}) will be calculated in the following section. When viewed from top, the position (x_{rd}, y_{rd}) from the center of the reflecting mirror to DMD can be calculated using z_{rd}, θ_t, and θ_a in Eqs. (1) and (2). To avoid interference between the reflecting mirror and optical components, z_{rd} was set to 200 mm. And the θ_t, tilt angle, is 24° because the micromirror is tilted at 12°. θ_a, the micromirror tilt axis, is 45° because the micromirror is a perfect square and it is tilted along its diagonal line. By substituting these values into Eqs. (1) and (2), the reflecting mirror position (x_{rd}, y_{rd}) becomes (62.96 mm, 62.96 mm).

$$x_{rd}=z_{rd}\cdot\tan\theta_t\cdot\cos\theta_a \quad (1)$$

$$y_{rd}=z_{rd}\cdot\tan\theta_t\cdot\sin\theta_a \quad (2)$$

3.2 Image-formation part

For the light reflected from DMD to be focused on the resin surface, the tube and objective lens are used for collimating and focusing the reflected light, respectively. The reflected light is assumed to be a set of point sources. Image-formation was simulated using ZEMAX, which is an optical design program that produces collimated light from a point source, and a focused image on the resin surface. In the simulation, the lens positions were optimized to reduce the diffraction effect and it was analyzed in the designed system. The quality of the focused image cannot be perfect due to aberrations and diffraction (Fischer and Tadic-Galeb, 2000). Aberrations, which are spherical aberration, astigmatism, coma, and chromatic aberration, distortion, and field curvature, occur due to the failure of the lens or optical system. When the light passes through the sharp edge or aperture, diffraction occurs and produces airy disk, which results in limiting resolving power of the image. In this research, an objective lens with 10 mm focal length (f_0) was used to produce a focused image. Using this lens is assumed to remove all aberrations, follow paraxial formulas, and consider only diffraction. The tube lens used to collimate rays emitted from point source of DMD is an achromat doublet with a 120 mm focal length, which is able to bring many colors to a common focus. Fig. 7(a) shows the position of the optimized tube lens when the image is formed for each ray. The point sources are assumed to be (0,0), (0,7), (5,7) on the DMD surface. OPD (Optical Path Difference), which is the difference between the real wavefront and a spherical reference wavefront, is one of the ways to measure the performance of the optical system. In the optical system, the diffraction at the limiting edge of the pupil will create an airy disk, which results in not forming the perfect image. Therefore if the average OPD along whole wavefront about one point

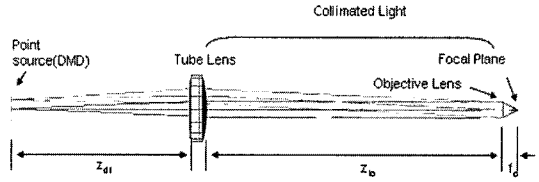

(a) Optimized layout for image-formation

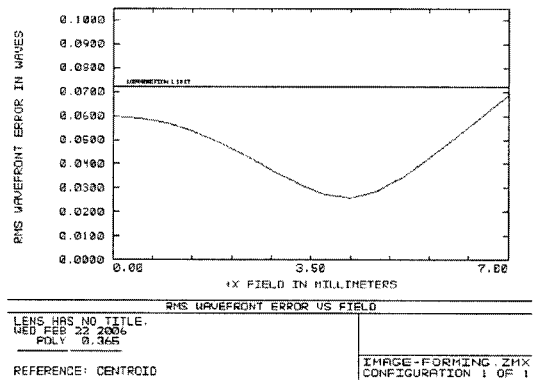

(b) RMS wavefront error

Fig. 7 Optical design using ZEMAX

source is below diffraction limit, the system can be said to diffraction-limited (Fischer and Tadic-Galeb, 2000). Fig. 7(b) shows the RMS wavefront error which means that the image forms under a diffraction limit from the 0 to 7 along the X axis in the simulation. The point source position (5,7) in the simulation is the border of DMD because the DMD is about 10.5mm×14.0 mm. Therefore, the image forms under a diffraction limit in the whole region of DMD. From the simulation, the optimized position for the tube lens (z_{dt}) is 115.2 mm, and for the objective lens (z_{to}) is 191 mm. The magnification of the designed optical system for image-formation is about 11.5 from the lens formula, z_{dt}/f_o.

3.3 System verification by measuring beam profile

To verify the illumination part, the forming image was observed on the beam profiler (BeamStar FX66, Ophir Optronics) after the convex lens was installed, and the 4 mm circular image was transferred to DMD. As shown in Fig. 8, the 2 mm image forms on the beam profiler by configuring the lens system with 1/2 magnification (m) using Eqs. (3) and (4), which are lens formulas. A con-

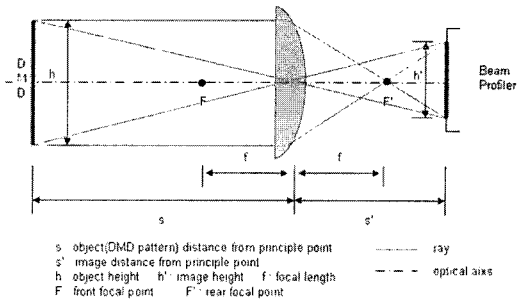

Fig. 8 Lens system for measuring beam profile

vex lens with a 70 mm focal length (f) was installed between DMD (object) and the beam profiler (image). DMD and the profiler are positioned at 210 mm (s) and 105 mm (s') from convex lens, respectively.

$$\frac{1}{f}=\frac{1}{s}+\frac{1}{s'} \tag{3}$$

$$m=\frac{s'}{s}=\frac{h'}{h} \tag{4}$$

Figure 9(a) and (b) show 2D and 3D profile respectively, that were measured by beam profiler. Fig. 9(c) shows section profiles along two perpendicular lines in Fig. 9(a). The measured diameter is bigger than 2 mm, which is the expected diameter in the optical design, because the optical defects such as aberrations and diffraction exist, and the positions of DMD and the beam profiler may be slightly off compared to the designed position. The measurement data is shown in Table 2. As can be seen, the measured intensity is relatively uniform and has an average intensity of about 14.7 mW/cm^2 and a standard deviation of about 1.127 mW/cm^2. In Table 2, the ellipticity represents that the alignment of the system can be acceptable for the fabrication of microstructures.

3.4 Fabrication resolution and system verification by fabricating 2D patterns

To measure the fabrication resolution of x and y direction, we made the 2D pattern as shown in Fig. 10. Fig. 10(a) shows 2D patterns which consist of long lines of 1 pixel to 4 pixels widths with the 1 pixel spacing increased from left to

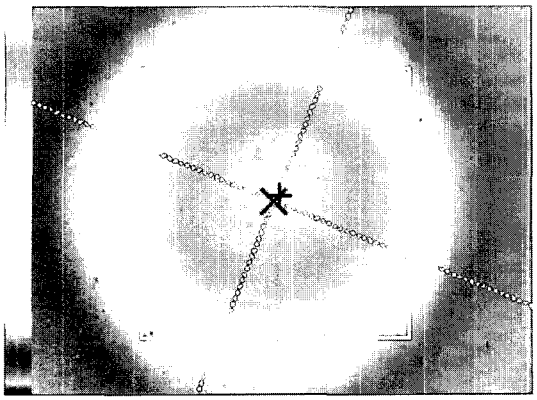

(a) 2D profile

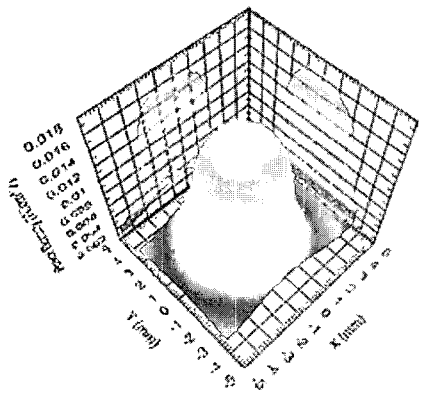

(b) 3D profile

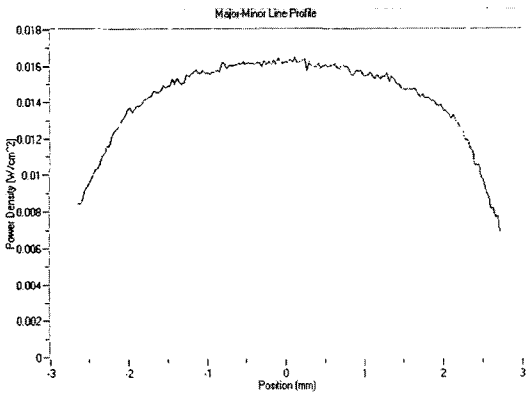

(c) Cross section profile of center line

Fig. 9 Measured profiles for the verification of alignment

right, respectively. Fig. 10(b) shows the fabricated patterns. It shows that 1 to 4 pixels lines can be fabricated, but some of lines were distorted or removed when rinsed using IPA. The fabrication resolution of x and y direction can be determined

Table 2 Measured data using beam profiler

Total power (mW)	3.08
Average intensity (mW/cm^2)	14.7
Standard deviation (mW/cm^2)	1.12
Ellipticity	0.992

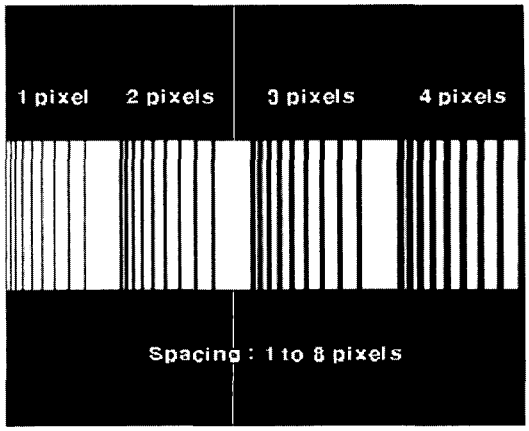

(a) 2D patterns image

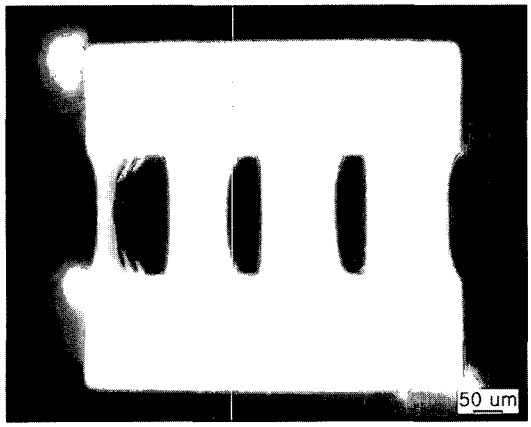

(b) Fabricated patterns

Fig. 10 2D pattern for x and y direction resolution

if neighboring lines with specified spacing were resolved. The lines with 1 and 2 pixels spacing in 4 cases weren't resolved. Therefore the resolution is 3 pixels and the real size is about 5 μm.

To verify the alignment of the illumination part and the focusing capability of image-formation part, 2D patterns were fabricated and measured using a microscope (DFC 280, LEICA). Fig. 11 (a) and (b) show photos of the fabricated grid pattern and characters, which represent the name

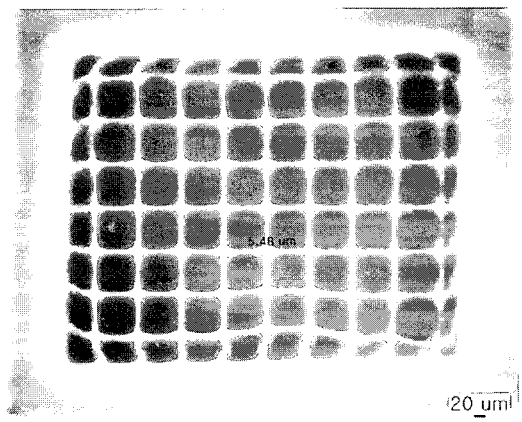

(a) Grid pattern

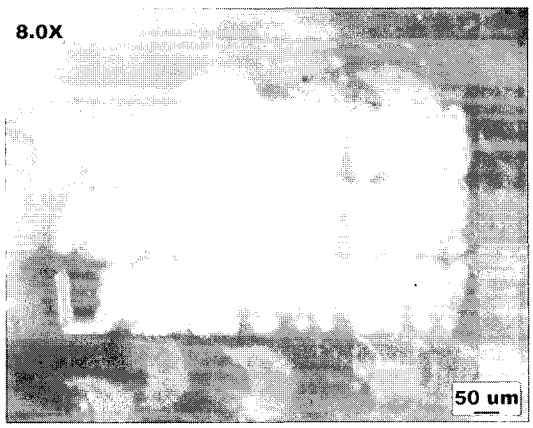

(b) Character pattern

Fig. 11 Photo of 2D pattern

of author's lab., respectively. The widths of the lines of grid and character patterns are about 5 μm and 20 μm, respectively. Therefore an image with a few μm resolution can be focused.

4. Fabrication of the 3D Microstructures

4.1 Material and control of stage movement

The Material used in this work is SOMOS 11120 (DSM Inc.), which has a viscosity of about 260 cps, which is considered low. The free surface technique is the method used to stack the fabricated layers. This method uses gravity of the resin and the movement of the Z stage to spread the resin. Therefore the lower viscosity the material has, the shorter the fabrication time is. As shown in Fig. 12, to quickly refresh the resin surface, the Z stage needs to go very far down in order to quickly cover the fabricated layer, and to go slowly upward to reach the layer thickness. The speed of the Z stage movement affects the total fabrication time. The speed of each step was empirically set to 100 mm/min. for a 2 mm downward movement, 30 mm/min. for a 1.5 mm upward movement, and 5 mm/min. for a 0.5 mm movement to the desired position. Three seconds are needed for the unstable resin surface to flatten. If the exposure time is one second, then the fabrication time for one layer is about 15 seconds.

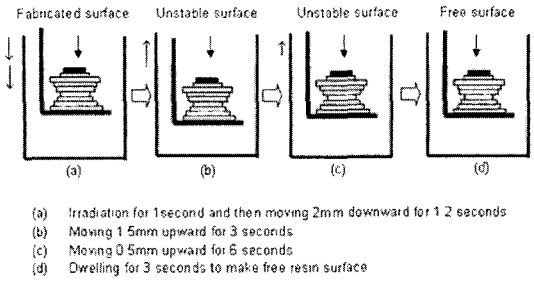

Fig. 12 Z stage movement to refresh resin surface

4.2 Fabrication examples

3D microstructures were fabricated using developed microstereolithography. Fig. 13 shows SEM photographs of a few 3D microstructures. The pyramid model as shown in Fig. 13(a) is 1000 μm$\times$ 1000 μm wide at the bottom layer and 2000 μm high. The layer thickness is 20 μm, the total layer number is 100, and the size of the top layer is about 30 μm wide. Fig. 13(b) shows round bar with high aspect ratio. The diameter and the height of the bar are about 120 μm and 2400 μm and aspect ratio is about 20. It consists of 80 layers with 30 μm layer thickness. The microfan 1 as shown in Fig. 13(c) is 300 μm high and the distance between the center of the fan and the end of the blade is about 550 μm. It consists of 60 layers with 5 μm layer thickness. The blade is about 40 μm wide. In Fig. 13(d) shows the same microfan as Fig. 13(c). The only different fabrication parameter is layer thickness, which is 20 μm, and it results in 1200 μm high.

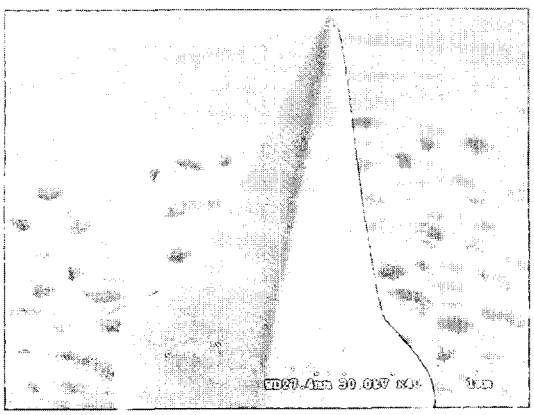

(a) Pyramid

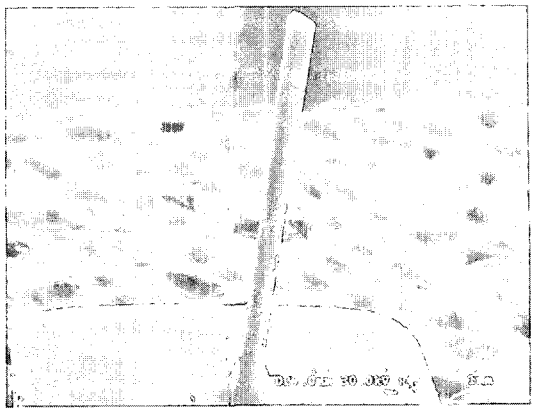

(b) Microneedle array

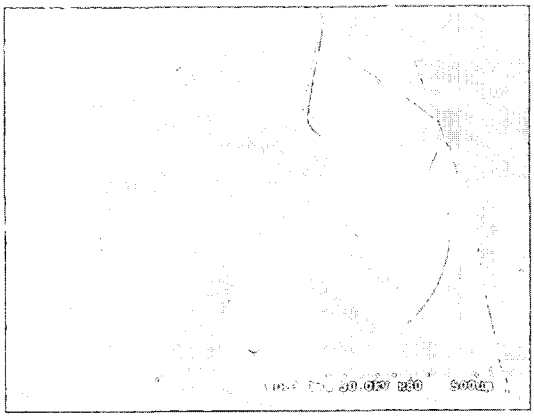

(c) Microfan 1

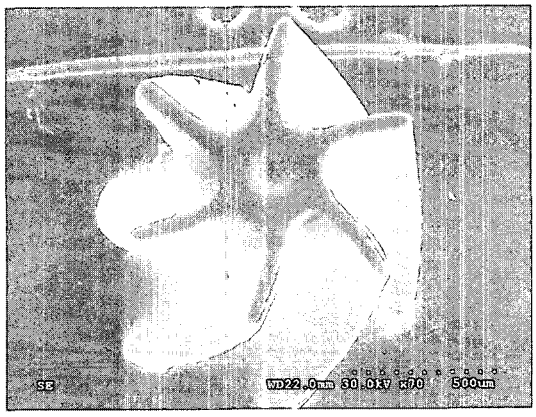

(d) Microfan 2

Fig. 13 Fabricated microstructures

Some fabricated microstructures have imperfection of the shape at the border because the energy distribution is not perfectly uniform. It would be solved by using microlens array called fly-eye type lens or total reflection light channel. In addition, unskillfulness of rinsing and post processing may affect the distortion of the fabricated microstructures.

5. Conclusions

A microstereolithography apparatus was developed in order to fabricate 3D microstructures. It consists of an illumination and image-formation part. The illumination part was designed to position each of the components so that the light would be incident onto DMD with uniform intensity after the light path was analyzed. The image-formation part was designed to position the tube and objective lens using an optical design program. In the designed system, it was known that the RMS front error about the position of any point source on DMD is under diffraction limit. To verify the designed system, the beam profiles and fabrications of a 2D pattern were measured and fabricated. The incident light on DMD was relatively uniform and the 2D patterned image was focused with a resolution of a few μm. Finally, 3D microstructures were fabricated with μm-sized features, complex shape, and high aspect ratios.

Acknowledgments

This work was supported by grant No. R01-2004-000-10507-0 from the Basic Program of the Korea Science & Engineering Foundation.

References

Bertsch, A., Jezequel, J. Y. and Andre, J. C., 1997, "Study of the Spatial Resolution of a New 3D Microfabrication Process: the Microstereophotolithography Using a Dynamic Mask-Generator Technique," *Journal of Photochemistry and Photobiology A : Chemistry* 107, pp. 275~281.

Bertsch, A., Bernhard, P., Vogt, C. and Renaud, P., 2000, "Rapid Prototyping of Small Size Objects," *Rapid Prototyping Journal*, Vol. 6, No. 4, pp. 259~266.

Bertsch, A., Jiguet, S. and Renaud, P., 2004, "Microfabrication of Ceramic Components by Microstereolithography," *Journal of Micromechanics and Microengineering*, Vol. 14, pp. 197~203.

Choi, J. W., Ha, M. Y., Won, M. H., Choi, K. H. and Lee, S. H., 2005, "Fabrication of 3-Dimensional Microstructures using Dynamic Image Projection," *Proceeding of the 1st International Conference on Precision Engineering and Micro/Nano Technology in Asia*, Shenzhen, China, pp. 472~476.

Farsari, M., Claret-Tournier, F., Huang, S., Chatwin, C. R., Budgett, D. M., Birch, P. M., Young, R. C. D. and Richardson, J. D., 2000, "A Novel High-Accuracy Microstereolithography Method Employing an Adaptive Electro-optic Mask," *Journal of Materials Processing Technology* 107, pp. 167~172.

Fischer, R. E. and Tadic-Galeb, B., 2000, *Optical System Design*, McGraw-Hill, pp. 35~47.

Ikuta, K. and Hirowatari, K., 1993, "Real Three Dimensional Micro Fabrication Using Stereolithography and Metal Molding," *Proceedings of the 6th IEEE Workshop on Micro Electro Mechanical Systems (MEMS'93)*, pp. 42~47.

Ikuta, K., Ogata, T., Tsuboi, M. and Kojima, S., 1996, "Development of Mass Productive Micro Stereo Lithography," *Proceedings of the 8th IEEE Workshop on Micro Electro Mechanical Systems (MEMS'96)*, Piscataway, NJ, USA, pp. 301~306.

Ikuta, K., Maruo, S. and Kojima, S., 1998, "New Micro Stereo Lithography for Freely Movable 3D Micro Structure — Super IH Process with Submicron Resolution," *Proceedings of the 11th IEEE Workshop on Micro Electro Mechanical Systems (MEMS'98)*, Heidelberg, Germany, pp. 290~295.

Ikuta, K., Maruo, S., Fujisawa, T. and Yamada, A., 1999, "Micro Concentrator with Opto-Sense Micro Reactor for Biochemical IC Chip Family — 3D Composite Structure and Experimental Verification," *Proceedings of the 12th IEEE Workshop on Micro Electro Mechanical Systems (MEMS '99)*, Orlando, Florida, USA, pp. 376~381.

Kim, D. S., Lee, I. H., Kwon, T. H. and Cho, D. W., 2005, "Development of a Three-Dimensional Barrier Embedded Kenics Micromixer by Means of a Micro-Stereolithography Technology," *Journal of KSME A*, Vol. 29, No. 6, pp. 904~912.

Lee, I. H., Cho, Y. H., Cho, D. W. and Lee, E. S., 2004, "Development of Micro-Stereolithography System for the Fabrication of Three-Dimensional Micro-Structures," *Journal of KSPE*, Vol. 21, No. 3, pp. 171~179.

Lee, I. H. and Cho, D. W., 2004, "An Investigation on Photopolymer Solidification Considering Laser Irradiation Energy in Micro-Stereolithography," *Microsystem Technologies*, Vol. 10, No. 8, pp. 592~598.

Limaye, A. S., 2004, *Design and Analysis of a Mask Projection Micro-Stereolithography System*, M.S. Thesis, Georgia Institute of Technology.

Maruo, S., Ikuta, K. and Korogi, 2003, "Force-Controllable, Optically Driven Micromachines Fabricated by Single-Step Two-Photon Microstereolithography," *Journal of Microelectromechanical Systems*, Vol. 12, No. 5, pp. 533~539.

Oda, G., Miyoshi, T., Takaya, Y., Ha, T. H. and Kimura, K., 2004, "Microfabrication of Overhanging Shape using LCD Microstereolithography," *5th International Symposium on Laser Precision Microfabrication, Proceedings of SPIE*, Vol. 5662, Bellingham, WA, pp. 649~654.

Park, S. H., Lim, T. W. and Yang, D. W., 2005, "Fabrication of Three-Dimensional Micro-Shell Structures Using Two-Photon Polymerization," *Journal of KSME A*, Vol. 29, No. 7, pp. 998~1004.

Park, S. H., Lim, T. W. and Yang, D. Y., 2006, "Investigation into Direct Fabrication of Nano-Patterns Using Nano-Stereolithography

(NSL) Process," *Journal of KSPE*, Vol. 23, No. 3, pp. 156~162.

Provin, C. and Monneret, S., 2002, "Complex Ceramic-Polymer Composite Microparts Made by Microstereolithography," *IEEE Transactions on Electronics Packaging Manufacturing*, Vol. 25, No. 1, pp. 59~63.

Smith, L. B., 2004, *Micro-Cross-Sectional Lithography (μCSL^{TM}) : Prototyping and Packaging for MEMS*, Ph. D. Thesis, Rensselaer Polytechnic Institute.

Sun, C. and Zhang, X., 2002, "Experimental and Numerical Investigations on Microstereolithography of Ceramics," *Journal of Applied Physics*, Vol. 92, No. 8, pp. 4796~4802.

Sun, C., Fang, N., Wu, D. M. and Zhang, X., 2005, "Projection Micro-Stereolithography Using Digital Micro-Mirror Dynamic Mask," *Sensors and Actuators A : Physical*, Vol. 121, Issue 1, 31, pp. 113~120.

Varadan, V. K., Jiang, X. and Varadan, V. V., 2001, *Microstereolithography and other Fabrication Techniques for 3D MEMS*, Wiley.

Zhang, X., Jiang, X. N. and Sun, C., 1999, "Micro-Stereolithography of Polymeric and Ceramic Microstructures," *Sensors and Actuators* 77, pp. 149~156.